ELSEVIER

Nuclear Medicine and Biology 28 (2001) 117–122

NUCLEAR MEDICINE — AND — BIOLOGY

Characterization of acetate metabolism in tumor cells in relation to cell proliferation: Acetate metabolism in tumor cells

Mitsuyoshi Yoshimoto[a], Atsuo Waki[a,*], Yoshiharu Yonekura[a], Norihiro Sadato[b], Tetsuhito Murata[c], Naoto Omata[a], Norio Takahashi[d], Michael J. Welch[e], Yasuhisa Fujibayashi[a]

[a]*Biomedical Imaging Research Center, Fukui Medical University, 23 Shimoaizuki, Matsuoka-cho, Yoshida-gun, Fukui, 910-1193, Japan*
[b]*National Institute for Physiological Sciences, Okazaki, Japan*
[c]*Department of Neuropsychiatry, Fukui Medical University, Fukui, Japan*
[d]*Department of Radiology, Fukui Medical University, Fukui, Japan*
[e]*Mallinckrodt Institute of Radiology, Washington University School of Medicine, St. Louis, Missouri 63110, USA*

Abstract

To reveal the metabolic fate of acetate in neoplasms that may characterize the accumulation patterns of [1-^{11}C]acetate in tumors depicted by positron emission tomography. Four tumor cell lines (LS174T, RPMI2650, A2780, and A375) and fibroblasts in growing and resting states were used. In uptake experiments, cells were incubated with[1-^{14}C]acetate for 40 min. [^{14}C]CO_2 was measured in the tight-air chamber, and the metabolites in cells were identified by thin layer chromatography and paper chromatography. The glucose metabolic rate of each cell line was measured with [2,6-^{3}H]2-deoxy-glucose (DG), and the growth activity of each cell line was estimated by measuring the incorporation of [^{3}H]methyl thymidine into DNA. Compared with resting fibroblasts, all four tumor cell lines showed higher accumulation of ^{14}C activity from [1-^{14}C]acetate. These tumor-to-normal ratios of [1-^{14}C]acetate were larger than those of DG. Tumor cells incorporated ^{14}C activity into the lipid-soluble fraction, mostly of phosphatidylcholine and neutral lipids, more prominently than did fibroblasts. The lipid-soluble fraction of ^{14}C accumulation in cells showed a positive correlation with growth activity, whereas the water-soluble and CO_2 fractions did not. These findings suggest that the high tumor-to-normal ratio of [1-^{14}C]acetate is mainly due to the enhanced lipid synthesis, which reflects the high growth activity of neoplasms. This in vitro study suggests that [1-^{11}C]acetate is appropriate for estimating the growth activity of tumor cells.

Keywords: Tumor; [1-^{14}C]Acetate; Lipid synthesis; Proliferation

1. Introduction

Radiolabeled acetate has long been used for the measurement of lipid and cholesterol synthesis in biochemistry [14,18]. Acetate is easily taken up by cells and converted to acetyl-CoA in both the cytosol and mitochondria by acetyl-CoA synthetase [2,3,12,13], a common metabolic intermediate for synthesis of cholesterol and fatty acids [21]. At the same time, acetyl-CoA is also a substrate for the TCA cycle [20].

Clinically, [1-^{11}C]acetate is a widely used positron emission tomography (PET) tracer for the evaluation of the myocardial oxidative metabolism [5,6,17]. In the case of normal myocardium, lipid metabolism, not glycolysis, is thought to be the major route for the production of large amounts of adenosine triphosphate (ATP), which is needed for myocardial contractile work. [1-^{11}C]acetate is rapidly taken up in the myocardium and subsequently metabolized to CO_2 via the TCA cycle. Considering the ratio between the initial uptake of [1-^{11}C]acetate and the remaining activity in the myocardium, most [1-^{11}C]acetate is metabolized to $^{11}CO_2$ (80% of total uptake, referred from [24]). Hence, converting [1-^{11}C]acetate to $^{11}CO_2$ via the TCA cycle is the dominant pathway in the myocardium.

Recently, [1-^{11}C]acetate has been reported to be a promising imaging tracer for tumors [24,25,28], especially in prostate cancer, in which tumors are not visualized clearly by FDG-PET because of the high renal clearance of FDG [27]. Using [1-^{11}C]acetate-PET, Shreve et al. [24] observed

*Corresponding author. Tel.: 81-776-61-8520; fax: 81-776-61-8151
E-mail address: Waki@fmsrsa.fukui-med.ac.jp (A. Waki).

0969-8051/01/$ – see front matter
PII: S0969-8051(00)00195-5

that renal cell carcinoma tissue demonstrates an initial high tracer uptake and much slower clearance of tissue tracer activity than dose non-neoplastic renal parenchyma. Although the mechanism of acetate accumulation in neoplasms is poorly known, the difference in clearance patterns suggests that the metabolic fate of acetate/acetyl-CoA in tumors is different from that in the myocardium. As proliferation is one of the most important characteristics of neoplasms, we hypothesize that the label is incorporated into membrane lipids in tumor cells. To test this hypothesis, we analyzed the metabolites of [1-^{11}C]acetate in 4 tumor cell lines and fibroblasts in growing and resting states. We compared the accumulation pattern of acetate with the glucose metabolism measured by [2,6-^{3}H]2-deoxy-glucose (DG) and the growth activity estimated by the incorporation of [^{3}H] methyl thymidine.

2. Materials and methods

2.1. Cell culture

Five cell lines were used, including LS174T: human colon adenocarcinoma, RPMI2650: human nasal septum quasi-diploid tumor, A2780: human ovary carcinoma, and A375: human malignant melanoma as tumor cell lines, and human fibroblasts were used as a normal cell line. All cell lines were purchased from Dai-Nippon Seiyaku Co. Ltd. (Japan) and maintained in a humidified atmosphere of 5% CO_2 in air at 37°C. LS174T and RPMI2650 were routinely maintained in Eagle's minimum essential medium (Nissui, Tokyo, Japan; 100 mg/dL glucose) supplemented with 1% non-essential amino acids and 10% fetal bovine serum. A2780 and A375 were maintained in Dulbecco's modified Eagle's medium (GIBCO BRL, NY, USA; 4.5 g/L glucose) supplemented with 10% fetal bovine serum. Fibroblasts were maintained in CS-C Complete Medium (Dai-Nippon Seiyaku Co. Ltd., Japan). At confluency, cells were dissociated with trypsin-ethylene diamine-tetraacetic acid (EDTA) (0.05% trypsin; 0.53mM EDTA). All cell studies were performed 24 hr after plating. In fibroblasts, a larger number of cells were plated when cells in the resting phase were used.

2.2. [1-^{14}C]acetate and [2,6-^{3}H]deoxyglucose uptake

Tumor cells and fibroblasts were trypsinized and plated in 24-well plates at a concentration of 2×10^5 and 10^6, respectively. Dulbecco's modified Eagle's medium was used as the assay medium. Five-hundred μl of assay medium containing 1μCi of [1-^{14}C]acetate or 2μCi of [2,6-^{3}H]deoxyglucose (DG) (Amersham, Tokyo, Japan) was added to each well. The plates with [1-^{14}C]acetate and [^{3}H]DG were incubated at 37°C for 40 min and 60 min, respectively. The medium was then removed and the cells were washed twice with ice-cold phosphate-buffered saline (PBS). Lysis was induced by adding 500 μl of 0.1N sodium hydroxide (NaOH). The whole lysates were then used for measurement of the radioactivity. After mixing lysates with a liquid scintillator (ACSII, Amersham), the radioactivity in lysates was measured with a liquid-scintillation counter (LSC-5000, Aloka, Tokyo, Japan).

2.3. [^{3}H]methyl thymidine incorporation into DNA

Tumor and fibroblast cells were seeded in 24-well plates at a concentration of 10^5 and 10^6, respectively. Cells were incubated with 500 μl of 0.5 μCi [^{3}H]methyl thymidine for 4 h. The medium was removed, and cells were washed twice with ice-cold PBS. One ml of 10% trichloroacetic acid (TCA) was added to the cells then the plates were placed on ice for 20 min. After the cells had been washed twice with 5% TCA, 0.5 ml of 0.5N NaOH was added and the cells were left on ice for 10 min. A 0.25 ml volume of 1N hydrochloric acid (HCl) was then added to the cells, mixing gently. Next, 0.25 ml of 40% TCA was added, again mixing gently, and the cells were placed on ice for 20 min. The insoluble material was filtrated on Whatman GF/C filters, and the filters were washed with ethanol (EtOH) three times. After drying, each filter was mixed with ACS II and measured for radioactivity.

2.4. Metabolism analysis

Tumor and fibroblast cells were seeded in 100mm dishes at a concentration of 2×10^6 and 2×10^7, respectively. To trap $^{14}CO_2$, the cells were incubated with 10 ml of 20 μCi [1-^{14}C]acetate in an tight-air chamber for 40 min. The chamber was connected to a collection vial through a nylon tube. The collection vials were filled with Carbo-Sorb E (Packard, Tokyo, Japan) to trap $^{14}CO_2$. After incubation for 40 min, the medium was removed to another dish and mixed with 0.1 ml of TCA to trap $^{14}CO_2$ in the medium (a modified method of [9]). The removed medium was incubated for an additional 15 min, and $^{14}CO_2$ was trapped in the Carbo-Sorb E. The radioactivity of $^{14}CO_2$ was measured by adding 9 ml of Permafluor E as a liquid scintillator to 1ml of Carbo-Sorb E. As a control experiment, the same procedure was conducted without cells. The net amount of $^{14}CO_2$ excreted from cells was calculated by subtracting the radioactivity in the no-cell control experiment from that in the experiments using cells.

After two washes with ice-cold PBS, 11.4 ml of 2 : 1 : 0.8 methanol : chloroform : water was added to the cells. Following the Bligh and Dyer extraction method [4], the radioactivity in the organic layer as the lipid-soluble fraction and in the water layer as the water-soluble fraction was measured. The organic and the water layers were concentrated at room temperature to about 100 μl under reduced pressure. Before evaporating the water layer, the water layer was alkalified by 0.1N NaOH to prevent possible evaporation of [1-^{14}C]acetate. Five μl of the concentrated organic

Table 1
The accumulation of radioactivity in cells

	Acetate	2-deoxyglucose
	(The ratio of tumor cells and growing fibroblasts to arrested fibroblasts)	
LS174T	1747.6 ± 112.7 (24.0)	381.0 ± 97.5 (4.3)
RPMI2650	1079.0 ± 83.1 (15.0)	608.5 ± 58.2 (6.8)
A2780	599.4 ± 79.5 (8.4)	298.2 ± 33.2 (3.3)
A375	283.4 ± 11.1 (4.0)	165.5 ± 6.1 (1.9)
Fibroblast	390.9 ± 39.8 (5.5)	184.0 ± 16.7 (2.1)
Fibroblast (arrest)	71.7 ± 2.1 (1.0)	89.3 ± 6.4 (1.0)

dpm/μg protein, mean ± SD. (n = 4)

layer was spotted on a silica gel G plate (Whatman, Tokyo, Japan) and lipids were separated by thin layer chromatography (TLC) using a solvent system consisting of chloroform : methanol : aqueous ammonium (210 : 90 : 7.5) to sort the lipids [7]. The lipids were identified by comparison with known standards. In the solvent system, lipids were separated as follows : phosphatidic acid (rate of flow (Rf) = 0.06 ± 0.003), phosphatidylserine-phosphatidylinositol (Rf = 0.12 ± 0.03), phosphatidylcholine (Rf = 0.41 ± 0.05), phosphatidylethanolamine (Rf = 0.50 ± 0.06), and neutral lipids near the solvent front. The lipids were detected by iodine vapor. An aliquot (7.5 μl) of the concentrated water layer was spotted on chromatography paper (anion exchanger, DE 81, Whatman). Using a solvent system containing water-saturated phenol : 0.05N sodium dihydrogen phosphate (10 : 0.5), which is a modification of the solvent system of Stark et al. [26], the water-soluble products, including acetate, acetyl-CoA, and amino acids, were separated as follows: acetate (Rf = 0.20 ± 0.05), acetyl-CoA (origin), amino acids (Rf = 0.88 ± 0.05). Amino acids were detected by spraying ninhydrin. To identify acetate and acetyl-CoA, [1-^{14}C]acetate and [1-^{14}C]acetyl-CoA were simultaneously developed. More than 80% of the [1-^{14}C]acetate spotted could be found on chromatography paper after separation. The plates and the papers were put on an imaging plate (BAS-MP 2040S, Fuji Photo Film Co.) and the exposed plate was scanned with a bio-imaging analyzer (BAS-1500, Fuji Photo Film Co.) to detect radioactivity.

3. Results

Compared with resting fibroblasts, all four tumor cell lines showed higher accumulation of ^{14}C activity from [1-^{14}C]acetate. These tumor-to-normal ratios of [1-^{14}C]acetate were larger than those of DG (Table 1).

Fig. 1 shows fractions of acetate metabolites by tumor cells and fibroblasts. In tumor cells, radioactivity derived from [1-^{14}C]acetate was mainly in the lipid-soluble fraction (55.7–82.7%, % of total accumulation in cells). Less radio-

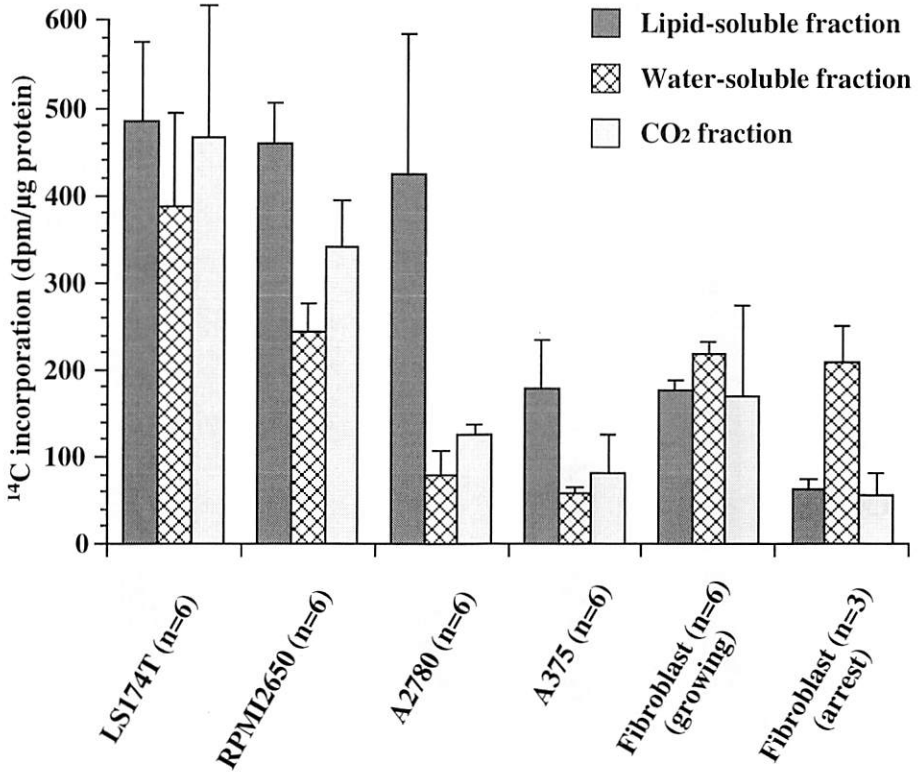

Fig. 1. Incorporation of [1-^{14}C]acetate into lipid-, water-soluble, and CO_2 fractions. Data represent mean ± SD.

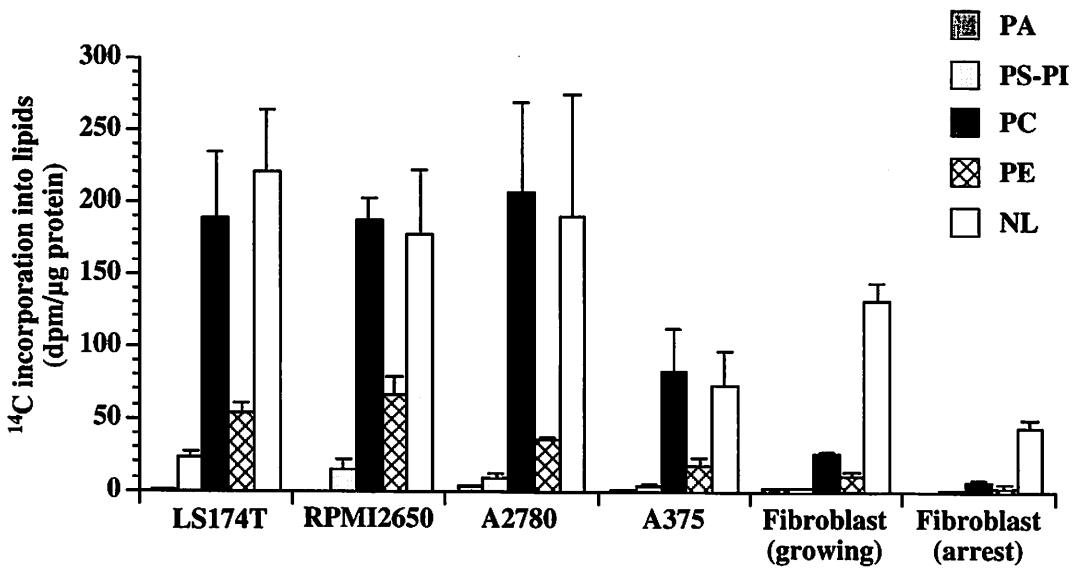

Fig. 2. Metabolic patterns of [1-^{14}C]acetate in lipid-soluble fraction. Data represent mean ± SD of 3–6 experiments. PA = phosphatidic acid, PS-PI = phosphatidylserine-phosphatidylinositol, PC = phosphatidylcholine, PE = phosphatidylethanolamine, NL = neutral lipids.

activity was found in water-soluble and CO_2 fractions. On the other hand, in fibroblasts, radioactivity derived from [1-^{14}C]acetate was mainly accumulated in the water-soluble fraction (55.1% in growing fibroblasts and 74.3% in resting fibroblasts).

In Fig. 2, it is clearly shown that phosphatidylcholine and neutral lipids were the main metabolites in the lipid-soluble fraction. The ratio of phosphatidylcholine to neutral lipids in tumor cells was larger than that in fibroblasts (1.17–0.86 in tumor cells, 0.20 in growing fibroblasts, and 0.15 in resting fibroblasts).

In all cells, over 85% of the radioactivity in the water-soluble fraction was in amino acids, with acetate and acetyl-CoA accounting for less than 13% of total activity (Fig. 3).

A significantly positive correlation was observed between total ^{14}C accumulation in cells and growth activity measured by [^{3}H]methyl thymidine incorporation into DNA ($y = 0.1525x - 89.763$, $r^2 = 0.8665$, $p = 0.0070$). The

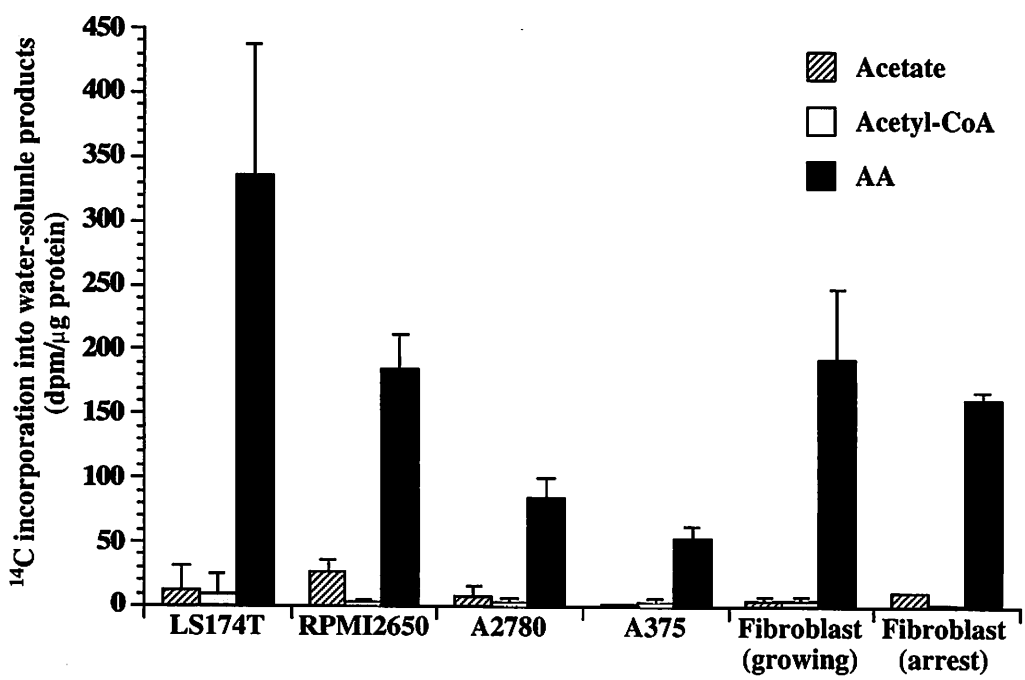

Fig. 3. Metabolic patterns of [1-^{14}C]acetate in water-soluble fraction. Data represent mean ± SD of 3–6 experiments. AA = amino acids.

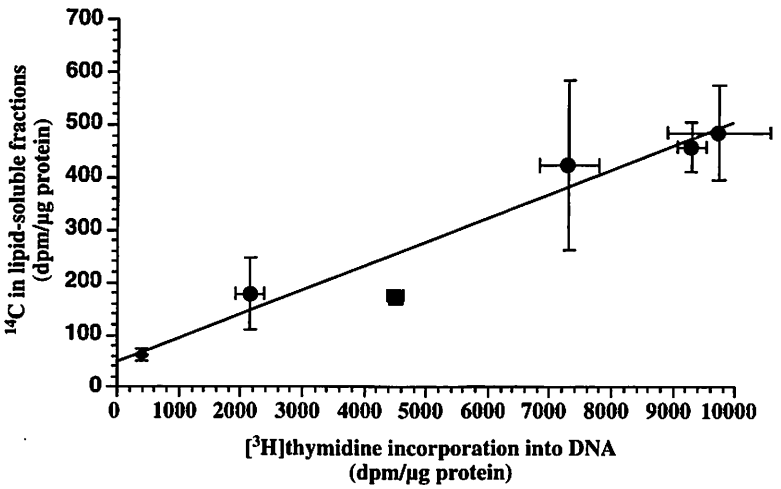

Fig. 4. Relation between ^{14}C in lipid-soluble fractions and [^{3}H]thymidine incorporation into DNA. There was a relationship between the two (p = 0.0016). Data represent the mean ± SD (n = 4). ● tumor cells; ◆, resting fibroblast; ■, growing fibroblast.

lipid-soluble fraction showed a positive correlation with the growth activity ($y = 0.462x + 43.235$, $r^2 = 0.9356$, $p = 0.0016$) (Fig. 4), whereas water-soluble fractions did not ($y = 0.0175x + 100.62$, $r^2 = 0.3287$, $p = 0.2342$), nor did CO_2 fractions ($y = 0.0330x + 31.856$, $r^2 = 0.6530$, $p = 0.0517$).

4. Discussion

The present study showed that tumor cells incorporate [1-^{14}C]acetate preferentially into the lipids rather than into the amino acids or CO_2. Given that acetate serves as a significant carbon source for lipid synthesis via acetyl-CoA [14,18], higher accumulation of ^{14}C in tumor cells may be due to enhanced lipid synthesis.

TLC analysis showed that phosphatidylcholine and neutral lipids are the main components of the lipid fraction in tumor cells. The ratios of phosphatidylcholine to neutral lipids in tumor cells were higher than those in fibroblasts. Both phosphatidylcholine and neutral lipids are contained in the cell membrane [15], and these lipids are essential for cell proliferation [8,11]. Phospholipids, especially phosphatidylcholine, are the major cellular constituents required for the assembly of biological membranes. Phosphatidylcholine is synthesized mainly through the CDP-choline pathway [16], in which choline kinase is a key enzyme. Choline kinase activity in mouse fibroblastic cells increases when the cells are transformed by oncogene [19,23]. This alternation in the phosphatidylcholine metabolism due to neoplastic transformation might partly explain the preferential incorporation of [1-^{14}C]acetate into phosphatidylcholine in tumor cells found in the present study.

The present study also showed that the retention of ^{14}C in the lipid-soluble fractions is correlated with growth activity. This is consistent with our hypothesis that acetate preferentially metabolizes to the membrane lipids in tumor cells, because cell growth and proliferation inevitably necessitate membrane constituents. Inhibition of DNA synthesis of HL-60 by dimethyl sulfoxide accompanied suppressed incorporation of [^{14}C]choline into phosphatidylcholine and [^{14}C]acetate into lipids [10]. The inhibition of phosphatidylcholine synthesis in A549 cells (lung carcinoma) induces apoptosis preceded by an arrest in the G0/G1 phase [22]. Considering these findings, acetate accumulation in neoplasms reflects their growth activity by enhancement of membrane synthesis.

Our results showed that [1-^{14}C]acetate was also incorporated into amino acids, and the levels of activity in the amino acid fraction were rather correlated with those in the CO_2 fraction. Glutamic acid and glutamine are the most abundant amino acids in tissues, and are known to be intermediate substrates in the TCA cycle [1]. Thus, the radiolabeled amino acids found in the present study are considered to be glutamic acid/glutamine. Under the condition of continuous [1-^{14}C]acetate input used in this study, production and degradation of intermediate metabolites in the TCA cycle were equilibrated, and could therefore be detected. In PET studies, in contrast, bolus injection of [1-^{11}C]acetate might allow us to visualize retentive lipid synthesis more selectively. Further in vivo analysis should be performed to clarify this point.

Higher tumor-to-normal ratios of [1-^{14}C]acetate in comparison with those of DG indicate the potential of [1-^{11}C]acetate to be a more sensitive tumor imaging tracer than [^{18}F]FDG. Given that this in vitro experiment differs from the in vivo system in several aspects such as blood flow and oxygen supply, further clinical evaluation is necessary.

References

[1] Badar-Goffer R. S., Bachelard H. S. and Morris P. G, Cerebral metabolism of acetate and glucose studied by 13C-NMR spectroscopy, Biochem J, 266, 133–139 (1990).

[2] Baranyai J. M. and Blum J. J, Quantitative analysis of intermediary metabolism in rat hepatocytes incubated in the presence and absence

of ethanol with a substrate mixture including ketoleucine, Biochem J, 258, 121–170 (1989).

[3] Barth C., Sladek M. and Decker K, Dietary changes of cytoplasmic acetyl-CoA synthetase in different rat tissues, Biochim Biophys Acta, 260, 1–9 (1972).

[4] Bligh E. G. and Dyer W. J, A rapid method for total lipid extraction and purification, Can J Biochem Physiol, 37, 911–918 (1959).

[5] Brown M., Marshall D. R., Sobel B. E. and Bergmann S. R, Delineation of myocardial oxygen utilization with carbon-11-labeled acetate, Circulation, 76, 687–696 (1987).

[6] Buxton D. B., Schwaiger M., Nguyen A., Phelps M. E. and Schelbert H. R, Radiolabeled acetate as a tracer of myocardial tricarboxylic acid cycle flux, Circ Res, 63, 628–634 (1988).

[7] Carderon P., Furnelle J. and Christophe J, In vitro metabolism in the rat pancreas I: basal lipid metabolism, Biochim Biophys Acta, 574, 379–390 (1979).

[8] Chen H.W, The activity of 3-hydroxy-3-metylglutaryl coenzyme A reductase and the rate of sterol synthesis diminish in cultures with high cell density, J Cell Physiol, 108, 91–97 (1981).

[9] Colquhoun A. and Curi R, Metabolic fate and effects of saturated and unsaturated fatty acids in Hep2 human larynx tumor cells, Biochem Mol Biol Int, 41, 597–607 (1997).

[10] Cooper R. A., Ip S. H. C., Cassileth P. A. and Kuo A. L, Inhibition of sterol and phospholipid synthesis in HL-60 promyelocytic leukemia cells by inducers of myeloid differentiation, Cancer Res, 41, 1847–1852 (1981).

[11] Cornell R., Grove G. L., Rothblat G. H. and Horwitz A.F, Lipid requirement for cell cycling, Exp Cell Res, 109, 299–307 (1977).

[12] Crabtree B., Gordon M. J. and Christie S. L, Measurement of the rates of acetyl-CoA hydrolysis and synthesis from acetate in rat hepatocytes and the role of these fluxes in substrate cycling, Biochem J, 270, 219–225 (1990).

[13] Goldberg R. P. and Brunengraber H, Contributions of cytosolic and mitochondrial acetyl-CoA syntheses to the activation of lipogenic acetate in rat liver, Adv Exp Med Biol, 132, 413–418 (1980).

[14] Howard B. V, Acetate as a carbon source for lipid synthesis in cultured cells, Biochim Biophys Acta, 488, 145–151 (1977).

[15] Howard B. V. and Howard W. J, Lipids in normal and tumor cells in culture, Prog Biochem Pharmacol, 10, 135–166 (1975).

[16] Kennedy E. P. and Weiss S. B, The function of cytidine coenzymes in the biosynthesis of phospholipids, J Biol Chem, 222, 193–214 (1956).

[17] Lear J. L, Relationship between myocardial clearance rates of carbon-11-acetate-derived radiolabel and oxidative metabolism: physiologic basis and clinical significance, J Nucl Med, 32, 1957–1960 (1991).

[18] Long V. J. W, Incorporation of 1-^{11}C-acetate into the lipids of isolated epidermal cells, Brit J Dermatology, 94, 243–252 (1976).

[19] Macara I. G, Elevated phosphocholine concentration in ras-transformed NIH 3T3 cells arises from increased choline kinase activity, not from phosphatidylcholine breakdown, Moll Cell Biol, 265, 6042–6047 (1989).

[20] Mayes P. A. (1996) The citric acid cycle: the catabolism of acetyl-CoA, Chapter 18. In: *Harper's Biochemistry*, 24th ed. (Edited by Murray R. K., Granner D. K., Mayes P. A. and Rodwell V. W.), pp. 168–175. Appleton & Lange. Stamford, CT.

[21] Mayes P. A. (1996) Biosynthesis of fatty acids, Chapter 23. In: *Harper's Biochemistry*, 24th ed. (Edited by Murray R. K., Granner D. K., Mayes P. A. and Rodwell VW.), pp. 216–223. Appleton & Lange. Stamford, CT.

[22] Miquel K., Pradines A., Tercé F., Selmi S. and Favre G, Competitive inhibition of choline phosphotransferase by geranylgeraniol and farnesol inhibits phosphatidylcholine synthesis and induces apoptosis in human lung adenocarcinoma A549 cells, J Biol Chem, 273, 26179–26186 (1998).

[23] Ratnan S. and Kent C, Early increase in choline kinase activity upon induction of the H-ras oncogene in mouse fibroblast cell lines, Arch Biochem Biophys, 323, 313–322 (1995).

[24] Shreve P. D., Chiao P.-C., Humes H. D., Schwaiger M. and Gross M. D, Carbon-11-acetate PET imaging in renal disease, J Nucl Med, 36, 1595–1601 (1995).

[25] Shreve P. D. and Gross M. D, Imaging of the pancreas and related disease with PET carbon-11-acetate, J Nucl Med, 38, 1305–1310 (1997).

[26] Stark J. B., Goodban A. E. and Owens H. S, Paper chromatography of organic acids, Anal Chem, 23, 413–415 (1951).

[27] Wahl R. L., Harney J., Hutchins G. and Grossman H. B, Imaging of renal cancer using positron emission tomography with 2-deoxy-2-(18F)-fluoro-D-glucose: pilot animal and human studies, J Urol, 146, 1470–1474 (1991).

[28] Yeh S. H., Liu R. S., Wu L. C., Yen S. H., Chang C. W. and Chen K. Y, ^{11}C-acetate clearance in nasopharyngeal carcinoma, Nucl Med Commun, 20, 131–134 (1999).